Supporting Information

Circularly polarized narrowband phosphorescent organic light-emitting diodes

Shaohua Wu [a, b#], Ping Chen [b, #], Xiaoyang Xia [c, #], Wenya Wang [a], Qifei Xie [b], Yanyu Qi [a, *], Huabo Han [d, *], Liang Zhou [c, *], and Guangzhao Lu [b, *]

[a] Hebei Key Laboratory of Organic Functional Molecules, Hebei Engineering Research Center of Thin Film Solar Cell Materials and Devices, College of Chemistry and Materials Science, Hebei Normal University, Shijiazhuang 050024, China.

[b] Shenzhen Institute of Information Technology, Shenzhen 518172, China.

[c] State Key Laboratory of Rare Earth Resource Utilization, Changchun Institute of Applied Chemistry, Chinese Academy of Sciences, Changchun 130022, China.

[d] Henan Key Laboratory of Biomolecular Recognition and Sensing, College of Chemistry and Chemical Engineering, Shangqiu Normal University, Shangqiu 476000, China.

[#] These authors contributed equally to this work.

Corresponding Authors

Yanyu Qi, Email: hbsdqyy@hebtu.edu.cn

Huabo Han, Email: 1412272575@qq.com

Liang Zhou, Email: zhoul@ciac.ac.cn

Guangzhao Lu, Email: lugz@sziit.edu.cn

1. General information

1.1 Materials and Measurements

All reagents and chemicals were purchased from commercial sources and used without further purification. ^{1}H NMR spectra were recorded by Bruker JEOL JNM-ECZ400S/L1 (400 MHz) spectrometers using DMSO-d6 as solvent and tetramethylsilane (TMS) as the internal standards. High resolution mass spectra (HRMS) were measured by Bruker MTQ III q-TOF

mass spectrometer. Thermo gravimetric analyses (TGA) were performed on a TGA2 (METTLER, Switzerland) instrument under nitrogen with a heating rate of 20 ^{o}C min^{-1}. Decomposition temperature (T_d, corresponding to 5% weight loss) of 374.6 ^{o}C was observed for Δ/Λ-(mpincz)$_2$Ir(*R*-camphor) phosphors. Absorption and photoluminescence spectra were measured on a UV-3100 spectrophotometer and a Hitachi F-7100 (HITACHI, Japan) photoluminescence spectrophotometer, respectively. The decay lifetimes and PLQY were measured with an Edinburgh Instruments FLS-1000 (England, Edinburgh) fluorescence spectrometer at room temperature. The absolute PLQYs were measured on a Quantaurus-QY measurement system equipped with a calibrated integrating sphere and all the samples were excited at 360 nm. The circular dichroism (CD) spectra were measured on a Jasco J-810 circular dichroism spectrometer with 'Low' sensitivity. The scan speed was set as 200 nm/min with 1 nm resolution and a respond time of 1.0 s. The circularly polarized photoluminescence (CPPL) spectra were measured on a Jasco CPL-300 spectrophotometer with 'Standard' sensitivity at 200 nm/min scan speed and respond time of 2.0 s employing "slit" mode.

1.2 X-ray Crystallography

The single crystal of the Δ-(mpincz)$_2$Ir(*R*-camphor) is obtained from slow evaporation of methanol/CH_2Cl_2 solution at room temperature. And the X-ray-diffraction data were carried out on a Bruker APEX2 SMART CCD diffractometer using monochromated Mo Kα radiation (λ = 0.71073 Å) at room temperature. Cell parameters were retrieved using SMART software and refined using SAINT on all observed reflections. Data were collected using a narrow-frame method with scan widths of 0.30° in ω and an exposure time of 10 s/frame. Crystal structures were solved by direct methods using the SHELXL-2018/3 software. None-hydrogen atoms were refined anisotropically by full-matrix least-squares calculations on F^2 using SHELXL-2018/3, while the hydrogen atoms were directly introduced at calculated position and refined in the riding mode.

1.3 Details of theoretical calculations and cyclic voltammetry measurements

Cyclic voltammograms (CV) were acquired in dichloromethane at room temperature with a CHI600e electrochemical analyzer (Chenhua, China) at 25 ^{o}C and a sweep speed of 100 mV s^{-1}. Tetrabutylammonium hexafluorophosphate (0.1 M) was applied as the supporting electrolyte. The conventional three-electrode configuration consisted of a platinum working electrode, a platinum wire auxiliary electrode and an Ag/Ag$^+$ reference electrode with

ferroceniumferrocene (Fc^+/Fc) as the internal standard. The HOMO energy levels of the compounds were calculated according to the formula: E_{HOMO} (eV) = - [4.8 + ($E_{1/2(ox/red)}$-$E_{1/2(Fc+/Fc)}$)] eV. The LUMO energy levels of the compounds were then deduced from the HOMO levels and the UV-Vis absorption on-sets of the longer wavelength.

We perform theoretical calculations employing Gaussian09 software with B3LYP function. The basis set of 6-31G(d, p) was used for C, H, N, O, and F atoms while the LanL2DZ basis set was employed for Ir atoms. The solvent effect of CH_2Cl_2 was taken into consideration using conductor like polarizable continuum model (C-PCM).

1.4 OLEDs fabrication and measurement

All the devices were grown on glass substrates pre-coated with a 180 nm thick layer of indium tin oxide (ITO) with a sheet resistance of 10 Ω per square. Before loading into the deposition system, the ITO substrates were pre-cleaned carefully and the surface was treated by oxygen plasma for 15 minutes. After UV ozone treatment, hole-injection material HATCN (6 nm) was firstly thermally deposited on, followed by the hole-transporting material HATCN (0.2%): TAPC (50 nm), emissive layer1 (the phosphors doped in the host TCTA, 10 nm), emissive layer2 (the phosphors doped in the host 26DCzPPy, 10 nm) and electron-transporting material Tm3PyP26PyB (60 nm). Finally, a cathode composed of lithium fluoride (LiF, 1 nm)/aluminum (Al, 100 nm) were sequentially deposited onto the substrate in the vacuum of 10^{-6} Pa. The current density-voltage-luminance (*J-V-L*) characteristics were measured using a Keithey 2400 Source meter and a Keithey 2000 Source multimeter equipped with a calibrated silicon photodiode. The EL spectra were measured by JY SPEX CCD3000 spectrometer. All measurements were carried out at room temperature under ambient conditions. The circularly polarized electroluminescence (CPEL) spectra were measured on a Jasco CPL-300 spectrophotometer with 'Standard' sensitivity at 200 nm/min scan speed and respond time of 2.0 s employing "slit" mode.

2. Experimental Section.

2.1 Synthetic routes for Δ/Λ-(mpincz)$_2$Ir(*R*-camphor).

2.1.1 Synthesis of main ligand 2-(6-methylpyridazin-3-yl)indolo[3,2,1-jk]carbazole.

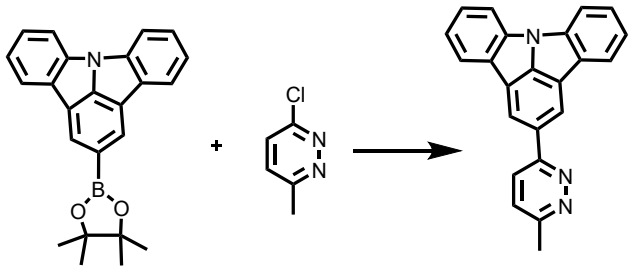

A mixture of 2-(4,4,5,5-tetramethyl-1,3,2-dioxaborolan-2-yl)indolo[3,2,1-jk]carbazole (1.2eq, 2g) and 3-chloro-6-methylpyridazine (1eq, 0.58g) in mixed solution of THF and 4M K_2CO_3 (2:1, v/v) was degassed before $Pd(PPh_3)_4$ (0.02eq, 0.125g) was added. And the mixture was refluxed under Ar for one day. After the reaction was finished, the organic layer was separated, washed with water, dried with Na_2SO_4, filtered and moved out with rotary evaporator. The residue was chromatographically purified on silica gel column with DCM/EA (5: 1, v/v) to give 2-(6-methylpyridazin-3-yl)indolo[3,2,1-jk]carbazole as a white solid (Yield：85%). Mass (HRMS): m/z, calcd. for $C_{23}H_{16}N_3^+$: 334.1344; found: 334.1348.

2.1.2 Synthesis of chiral iridium(III) complexes Δ/Λ-(mpincz)$_2$Ir(*R*-camphor).

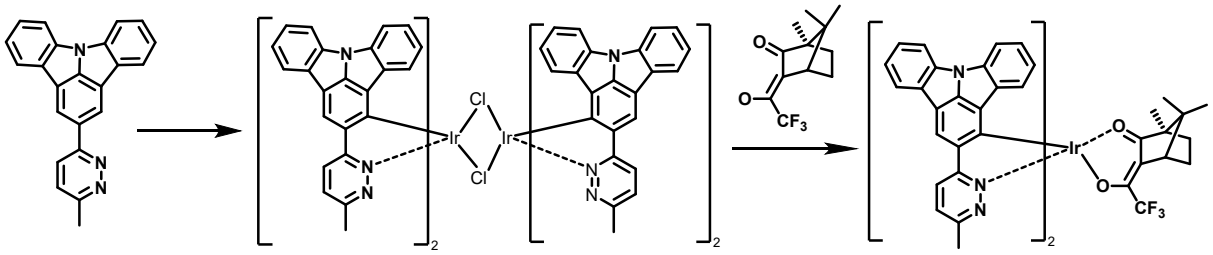

Δ/Λ -(mpincz)$_2$Ir(*R*-camphor)

The $IrCl_3$ (0.26 g, 0.75 mmol) and 2.4 equivalent of cyclometalated ligand (0.6 g, 1.80 mmol) were added in a 2-ethoxyethanol and water mixture. Then, the solution was heated for 16 h at 110 °C. After the addition of water, precipitated yellow powder of $[(C^\wedge N)_2Ir(\mu\text{-}Cl)]_2$ chloridebridged dimmer was filtered and reacted with *R*-camphor for 12 h at 110 °C. The solution was concentrated and the resulting residue was purified by silica gel column chromatography CH_2Cl_2 and vacuum sublimation gave yellow power. (Yield：60%). The isomers Δ/Λ-(mpincz)$_2$Ir(*R*-camphor) are separated into Δ-(mpincz)$_2$Ir(*R*-camphor) and Λ-(mpincz)$_2$Ir(*R*-camphor) by chiral column chromatography, respectively.

Δ-(mpincz)$_2$Ir(*R*-camphor): ^{1}H NMR (400 MHz, DMSO-d_6) δ 9.08 (s, 1H), 9.05 (s, 1H), 8.97 (dd, *J* = 9.1, 3.6 Hz, 2H), 8.21 (dd, *J* = 7.7, 3.2 Hz, 2H), 8.13 (d, *J* = 8.4 Hz, 2H), 8.01 (d, *J* = 8.0 Hz, 2H), 7.96 (d, *J* = 7.7 Hz, 2H), 7.51 (t, *J* = 7.9 Hz, 2H), 7.39 (dt, *J* = 7.9, 3.8 Hz, 2H), 7.23 (d, *J* = 7.7 Hz, 2H), 6.65 (td, *J* = 7.9, 4.2 Hz, 2H), 6.26 (dd, *J* = 13.1, 8.1 Hz, 2H), 2.41 (s, 3H), 2.35 (s, 3H), 1.49 (s,

1H), 1.31 (d, J = 15.0 Hz, 4H), 0.74 (s, 3H), 0.50 (s, 3H), 0.35 (s, 3H). Mass (HRMS): m/z, calcd. for $C_{58}H_{43}F_3IrN_6O_2^+$: 1105.3029; found: 1105.3035.

Λ-(mpincz)$_2$Ir(R-camphor): ^{1}H NMR (400 MHz, DMSO-d_6) δ 9.08 (s, 1H), 9.05 (s, 1H), 8.97 (dd, J = 9.1, 3.6 Hz, 2H), 8.21 (dd, J = 7.7, 3.2 Hz, 2H), 8.13 (d, J = 8.4 Hz, 2H), 8.01 (d, J = 8.0 Hz, 2H), 7.96 (d, J = 7.7 Hz, 2H), 7.51 (t, J = 7.9 Hz, 2H), 7.41 - 7.36 (m, 2H), 7.24 (t, J = 7.8 Hz, 2H), 6.66 (td, J = 7.4, 3.7 Hz, 2H), 6.26 (dd, J = 13.1, 8.1 Hz, 2H), 2.41 (s, 3H), 2.35 (s, 3H), 1.49 (s, 1H), 1.31 (d, J = 15.0 Hz, 4H), 0.74 (s, 3H), 0.50 (s, 3H), 0.35 (s, 3H). Mass (HRMS): m/z, calcd. for $C_{58}H_{43}F_3IrN_6O_2^+$: 1105.3029; found: 1105.3027.

Figures and Tables

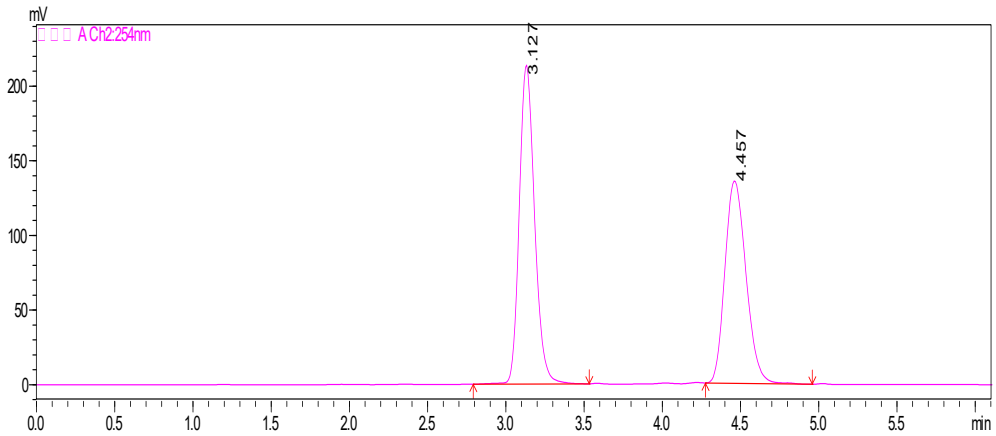

	RT	Area	%Area	Height
1	3.127	1454735	53.36	213743
2	4.457	1271417	46.64	135587

Fig. S1 The chiral HPLC profile of Δ/Λ-(mpincz)$_2$Ir(R-camphor).

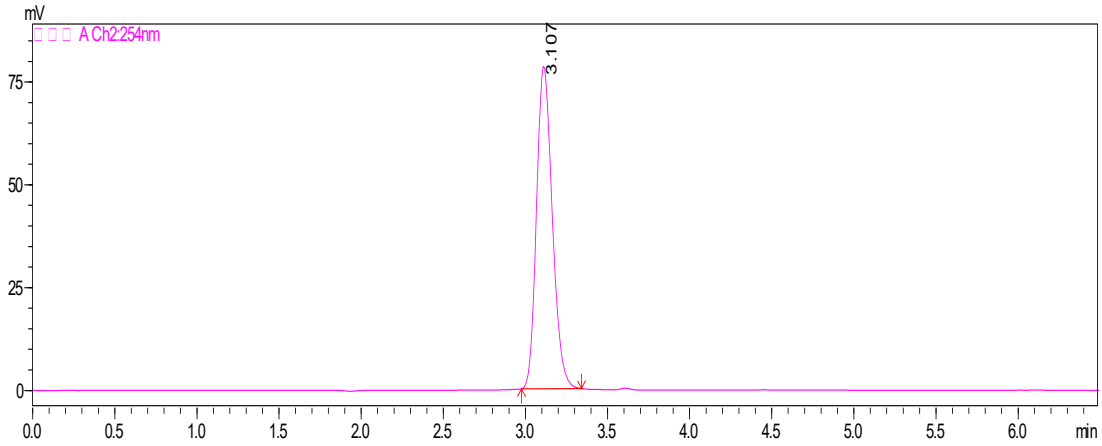

	RT	Area	%Area	Height
1	3.107	524585	100	78339

Fig. S2 The chiral HPLC profile of Δ-(mpincz)$_2$Ir(*R*-camphor).

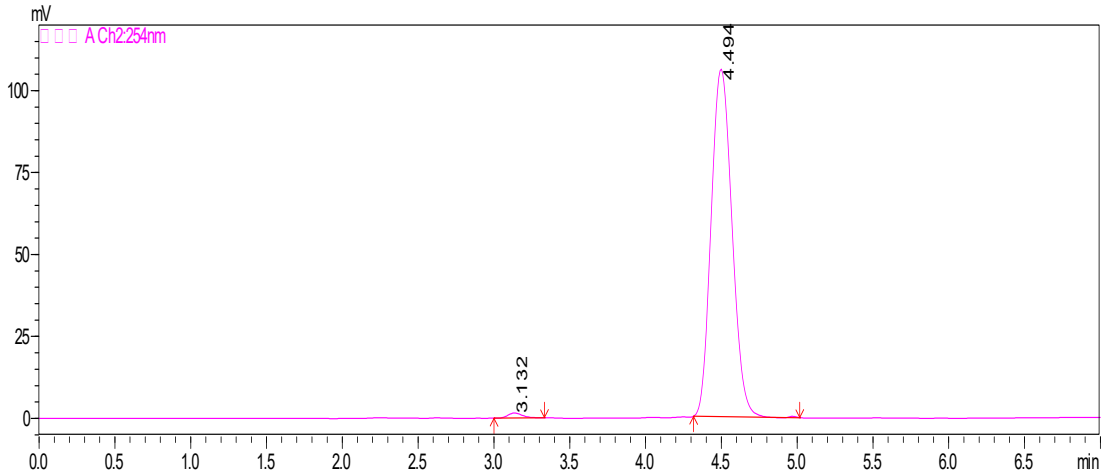

	RT	Area	%Area	Height
1	3.132	9996	0.98	1542
2	4.494	1011568	99.02	106.059

Fig. S3 The chiral HPLC profile of Λ-(mpincz)$_2$Ir(*R*-camphor).

Display Report

Analysis Info

Analysis Name	D:\Data\DATA\DATA-WJJ\SZXX\20231109\SZXX-MS-20231109003000002.d	Acquisition Date	11/9/2023 3:15:16 PM
Method	DirectInfusion_TuneLow_pos.m	Operator	bruker
Sample Name	9#	Instrument	micrOTOF-Q III 8228888.20519
Comment			

Acquisition Parameter

Source Type	ESI	Ion Polarity	Positive	Set Nebulizer	0.4 Bar
Focus	Active	Set Capillary	4500 V	Set Dry Heater	180 °C
Scan Begin	50 m/z	Set End Plate Offset	-500 V	Set Dry Gas	4.0 l/min
Scan End	1000 m/z	Set Collision Cell RF	140.0 Vpp	Set Divert Valve	Waste

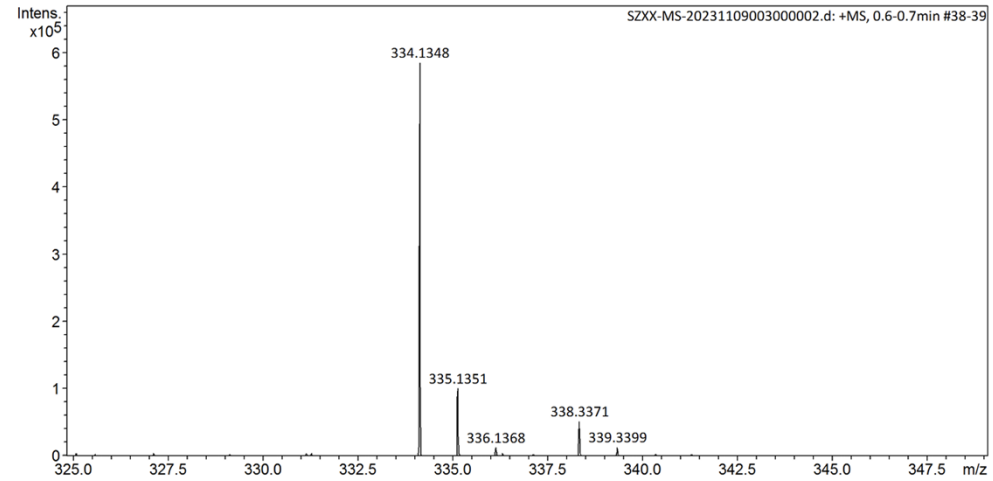

Fig. S4 The HR-MS spectrum of 2-(6-methylpyridazin-3-yl)indolo[3,2,1-jk]carbazole.

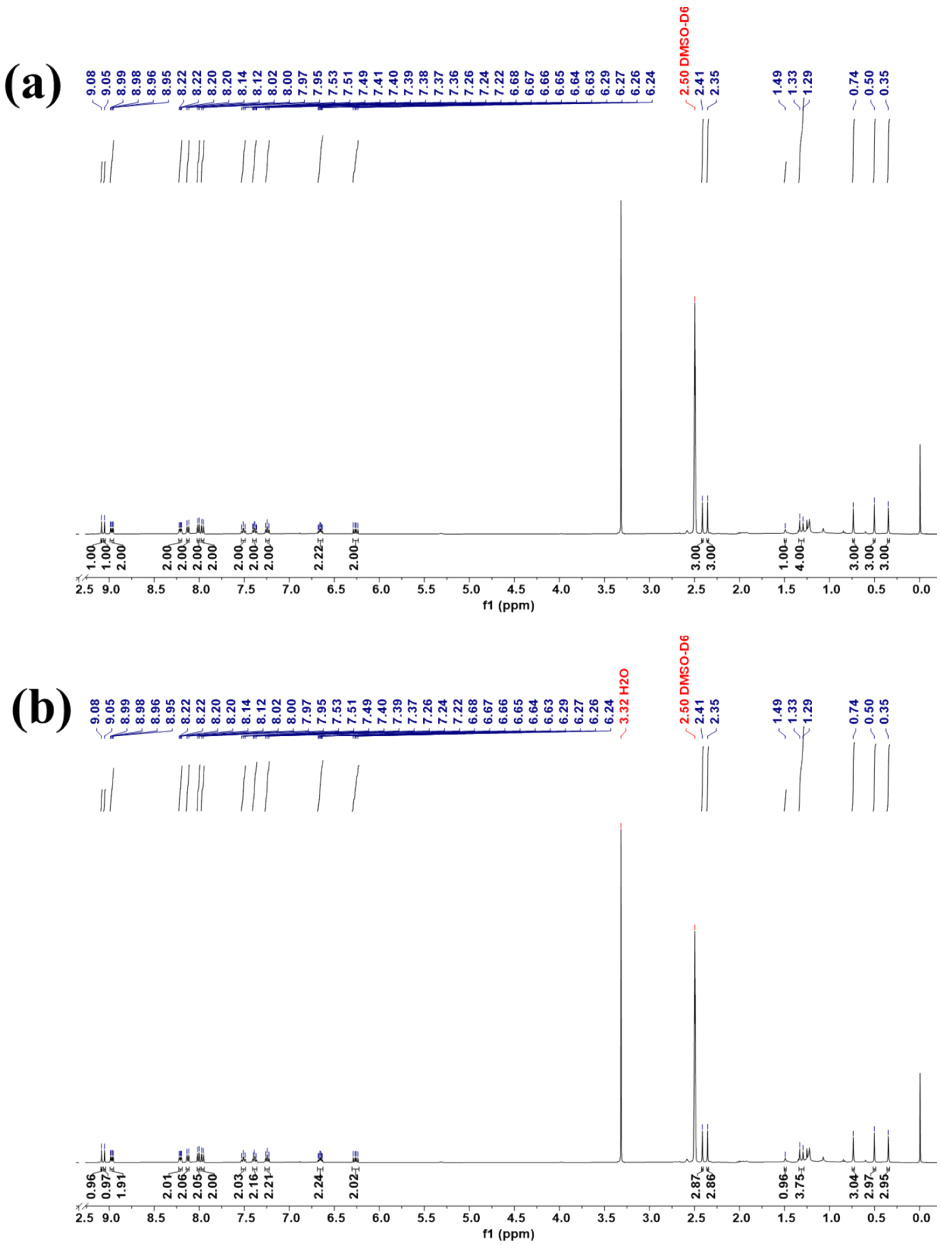

Fig. S5 The ^{1}H NMR spectrum in DMSO-d6: (a) for Δ-(mpincz)$_2$Ir(*R*-camphor); (b) for Λ-(mpincz)$_2$Ir(*R*-camphor).

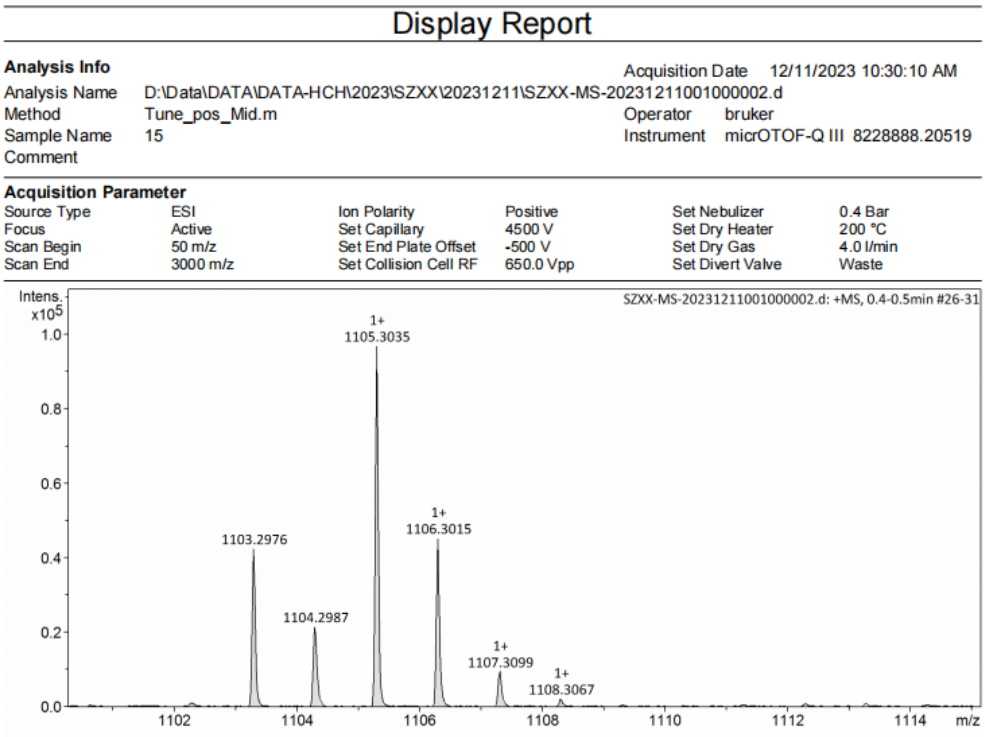

Fig. S6 The HR-MS spectrum of Δ-(mpincz)$_2$Ir(*R*-camphor).

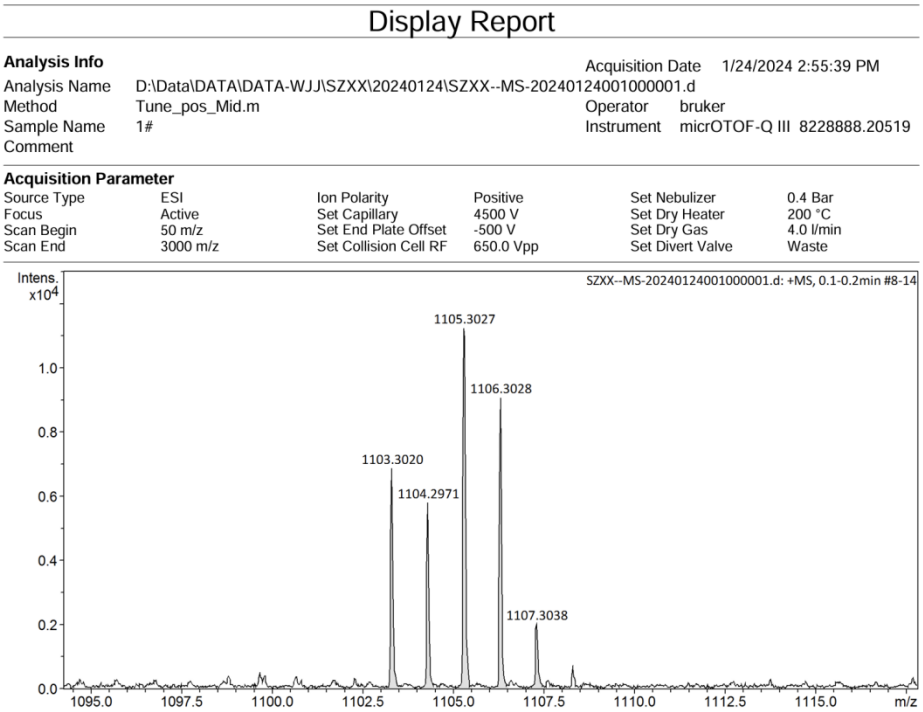

Fig. S7 The HR-MS spectrum of Λ-(mpincz)$_2$Ir(*R*-camphor).

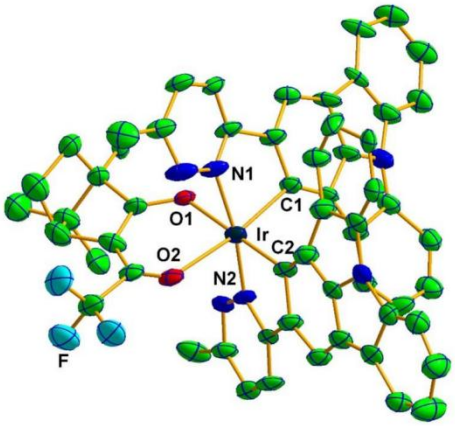

Fig. S8 The crystal structure of Δ-(mpincz)$_2$Ir(*R*-camphor).

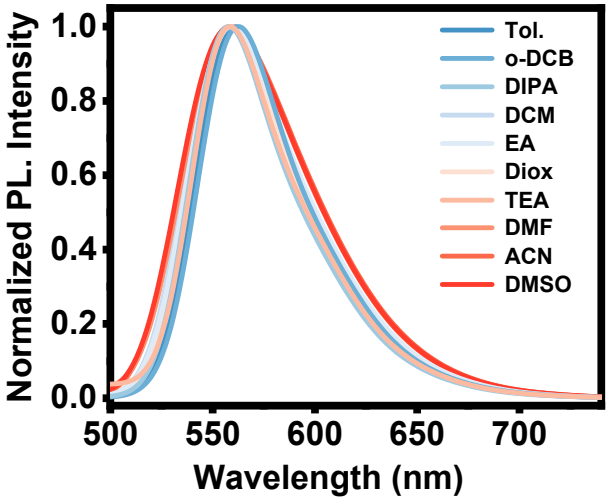

Fig. S9 The photoluminescence spectra of Δ/Λ-(mpincz)$_2$Ir(*R*-camphor) recorded in solvents of distinctive polarity.

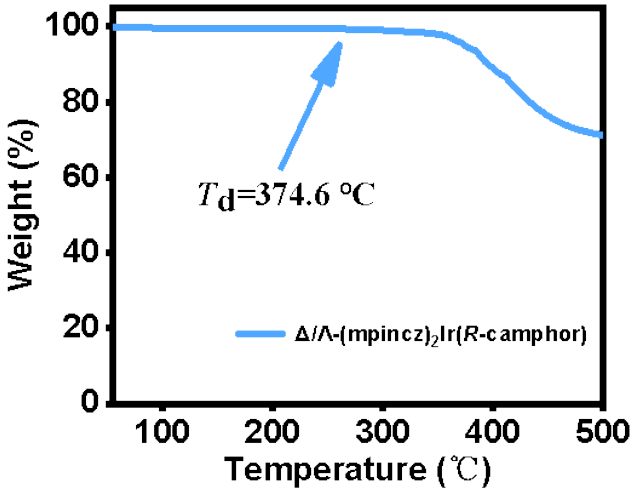

Fig. S10 Thermal gravimetric analysis (TGA) curves of Δ/Λ-(mpincz)$_2$Ir(*R*-camphor).

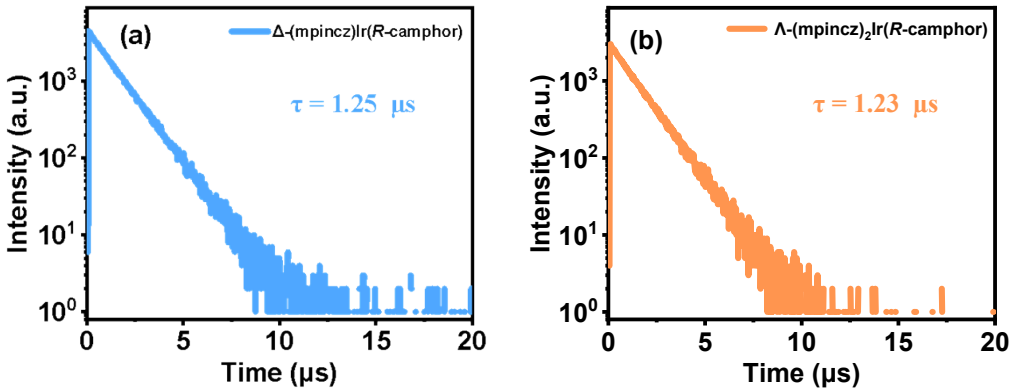

Fig. S11 The lifetime curves of chiral iridium complexes in degassed toluene solution.

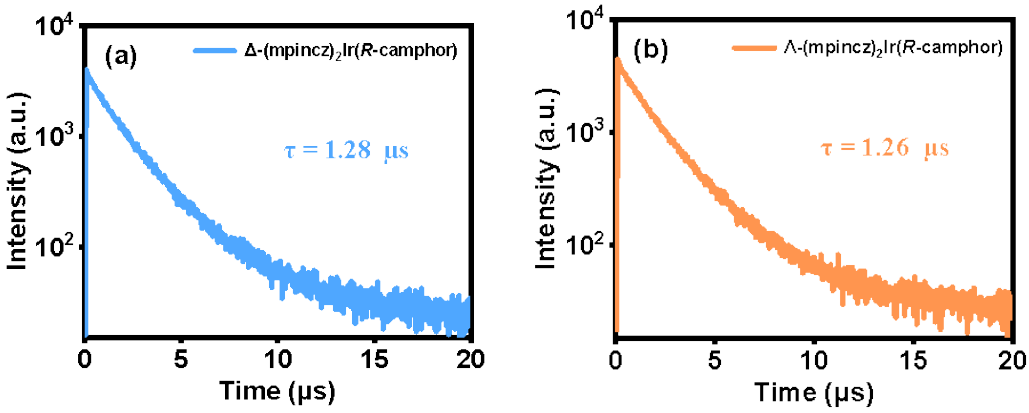

Fig. S12 The lifetime curves of chiral iridium complexes in 6 wt% TCTA doped films by evaporation.

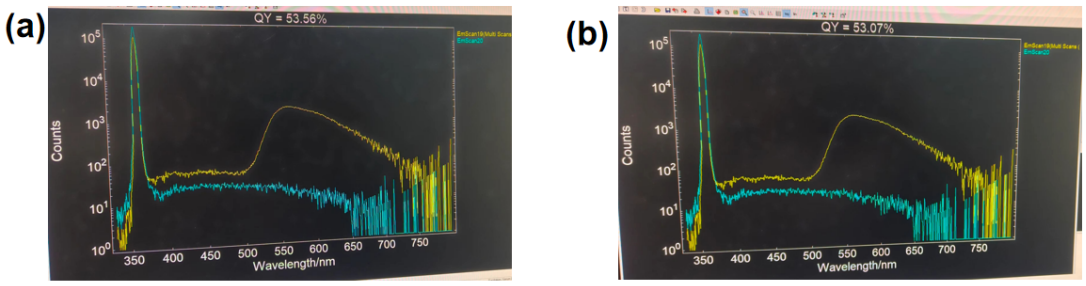

Fig. S13 The PLQYs of the isomers in 6 wt% TCTA doped films by evaporation: (a) for Δ-(mpincz)$_2$Ir(*R*-camphor); (b) for Λ-(mpincz)$_2$Ir(*R*-camphor).

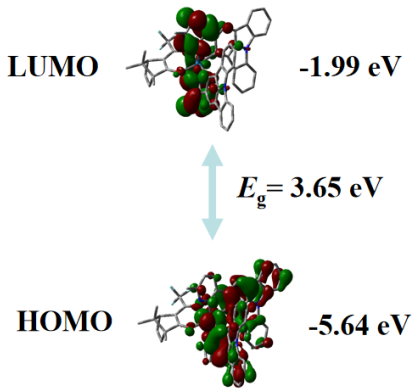

Fig. S14 The isodensity surface plots and HOMO/LUMO orbital levels of Δ/Λ-(mpincz)$_2$Ir(*R*-camphor).

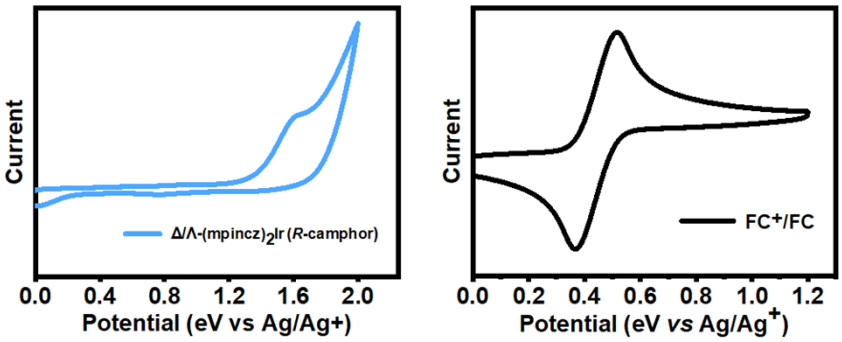

Fig. S15 The cyclic voltammograms of complex Δ/Λ-(mpincz)$_2$Ir(*R*-camphor).

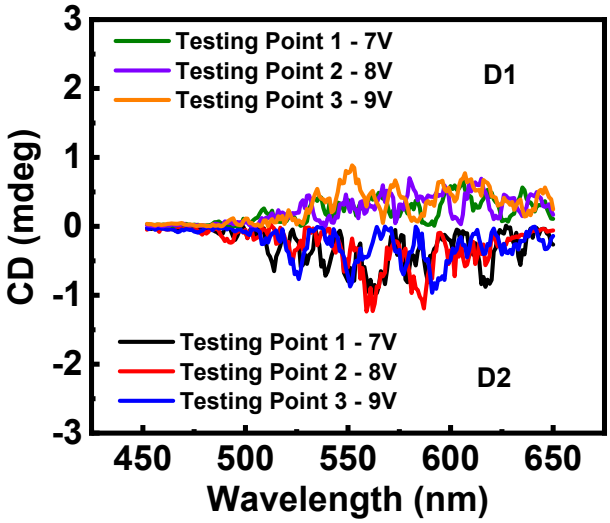

Fig. S16 The CPEL plots of three different testing points of devices D1 and D2, which were measured at different voltages of 7 V, 8 V, and 9V, respectively.

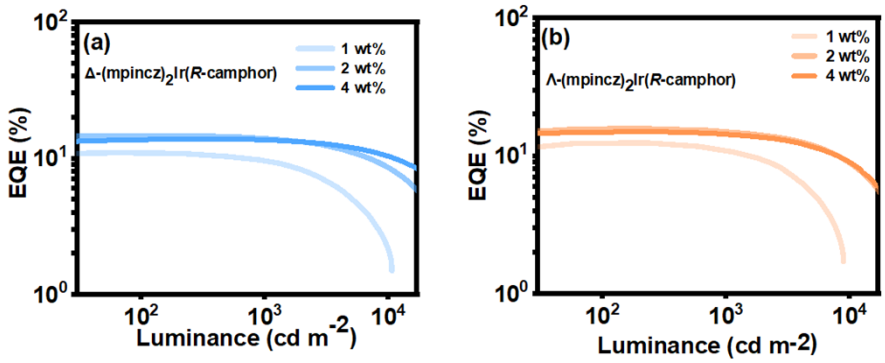

Fig. S17 The EQE - luminance curves based on Δ/Λ-(mpincz)$_2$Ir(*R*-camphor) with different doping concentrations: (a) for Δ-(mpincz)$_2$Ir(*R*-camphor); (b) for Λ-(mpincz)$_2$Ir(*R*-camphor).

Table. S1 Crystal data and structure refinement for Δ-(mpincz)$_2$Ir(*R*-camphor).

Identification code	Δ-(mpincz)$_2$Ir(*R*-camphor)
Empirical formula	$C_{61}H_{48}Cl_6F_3IrN_6O_2$
Formula weight	1358.95
Temperature/K	223.00
Crystal system	monoclinic
Space group	$P2_1$
a/Å	17.2107(5)
b/Å	17.8095(4)
c/Å	18.4348(3)
α/°	90
β/°	92.706(2)
γ/°	90
Volume/Å^3	5644.2(2)
Z	4
ρ_{calc}g/cm^3	1.599
μ/mm^{-1}	7.689
F(000)	2712.0
Crystal size/mm^3	0.15 × 0.13 × 0.12
Radiation	Cu Kα (λ = 1.54178)
2Θ range for data collection/°	4.798 to 138.13
Index ranges	$-20 \leq h \leq 20$, $-17 \leq k \leq 21$, $-17 \leq l \leq 22$
Reflections collected	35867
Independent reflections	16919 [R_{int} = 0.0443, R_{sigma} = 0.0598]
Data/restraints/parameters	16919/155/1488
Goodness-of-fit on F^2	1.049
Final R indexes [I>=2σ (I)]	R_1= 0.0365, wR_2= 0.0865
Final R indexes [all data]	R_1= 0.0413, wR_2= 0.0901
Largest diff. peak/hole / e Å^{-3}	0.74/-0.97

Flack parameter	0.017(8)

Table. S2 The electronic cloud density distribution.

Complex	Orbital	Energy/eV (Calculated)	Energy/eV (Experiment)	Composition (%)		
				Main ligand	Ir	Ancillary Ligand
Δ/Λ-(mpincz)$_2$Ir(*R*-camphor)	HOMO	-5.64	-5.56	70.3	26.8	2.7
	LUMO	-1.99	-3.18	94.2	4.2	1.6